Article Type: Letters

Soil fertility shapes belowground food webs across a regional climate gradient

Etienne Laliberté[1,2,†], Paul Kardol[3*†], Raphael K. Didham[2,4], François P. Teste[2,5], Benjamin L. Turner[6], David A. Wardle[3,7]

[1] Centre sur la biodiversité, Institut de recherche en biologie végétale, Département de sciences biologiques, Université de Montréal 4101 Sherbrooke Est, Montréal, Québec H1X 2B2, Canada

[2] School of Biological Sciences, The University of Western Australia, 35 Stirling Highway, Crawley, Perth, WA 6009, Australia

[3] Department of Forest Ecology & Management, Swedish University of Agricultural Sciences, SE-901 83, Umeå, Sweden

[4] CSIRO Land & Water, Centre for Environment and Life Sciences, 147 Underwood Avenue, Floreat, Perth, WA 6014, Australia

[5] Grupo de Estudios Ambientales, IMASL-CONICET & Universidad Nacional de San Luis, Av. Ejército de los Andes 950 (5700), San Luis, Argentina

[6] Smithsonian Tropical Research Institute, Apartado 0843-03092, Balboa, Ancon, Republic of Panama

[7] Asian School of the Environment, Nanyang Technological University, Singapore 639798

*Corresponding author. Email: paul.kardol@slu.se

Phone: +46-90-786 8398

Fax: +46-90-786 8163

[†]Equal contribution.

E-mail addresses: Etienne Laliberté: etienne.laliberte@umontreal.ca; Paul Kardol: Paul.Kardol@slu.se; Raphael Didham: Raphael.Didham@csiro.au; François Teste: francois.teste@uwa.edu.au; Benjamin Turner: TurnerBL@si.edu; David Wardle: David.Wardle@slu.se

This is the author manuscript accepted for publication and has undergone full peer review but has not been through the copyediting, typesetting, pagination and proofreading process, which may lead to differences between this version and the Version of Record. Please cite this article as doi: 10.1111/ele.12823

Statement of authorship: EL, PK, DAW designed the study, and all authors collected data. EL, PK, DAW analyzed data and wrote the first draft of the manuscript, and all authors contributed substantially to revisions.

Running title: Soil fertility, climate and soil food webs

Keywords: bacteria, climate, energy channel, fungi, microarthropod, nematode, pedogenesis, precipitation, succession, retrogression

Type of article: Letter

Number of words: 149 (abstract), 5013 (main text, excluding abstract, acknowledgements references, table and figure legends).

Number of references: 60
Number of figures: 6
Number of tables: 0

Abstract

Changes in soil fertility during pedogenesis affect the quantity and quality of resources entering the belowground subsystem. Climate governs pedogenesis, yet how climate modulates responses of soil food webs to soil aging remains unexplored because of the paucity of appropriate model systems. We characterized soil food webs along each of four retrogressive soil chronosequences situated across a strong regional climate gradient to show that belowground communities are predominantly shaped by changes in fertility rather than climate. Basal consumers showed hump-shaped responses to soil aging, which were propagated to higher-order consumers. There was a shift in dominance from bacterial to fungal energy channels with increasing soil age, while the root energy channel was most important in intermediate-aged soils. Our study highlights the overarching importance of soil fertility in regulating soil food webs, and indicates that belowground food webs will respond more strongly to shifts in soil resources than climate change.

INTRODUCTION

Local scale variation in soil fertility, notably the availability and supply of nutrients, is a fundamental driver of community and ecosystem properties (Grime 2001; Vitousek 2004). Both

aboveground and belowground communities frequently show coordinated responses to spatial variation in soil fertility, because fertility regulates the quantity and quality of plant-derived resources that enter the soil, which in turn impacts the soil biota that influence plant nutrition and growth through both indirect and direct pathways (Berendse 1998; Wardle *et al.* 2004a; van der Putten *et al.* 2013). Soil age can be an important driver of this spatial variation. Notably, chronosequences that are of sufficient duration to include stages that have undergone ecosystem retrogression (i.e., declines in ecosystem level processes including plant productivity and decomposition), due to losses in soil nutrients over geological time scales, offer important insights into the ecological effects of changes in soil fertility (Walker & Syers 1976; Vitousek 2004; Wardle *et al.* 2004b; Peltzer *et al.* 2010). Studies of long-term chronosequences have shown that soil fertility and primary productivity initially increase up to a peak during the early 'build-up' phase of ecosystem development due to increases in nitrogen (N) availability, but then gradually decline due to losses of rock-derived nutrients, notably phosphorus (P) (Wardle et al. 2004, Peltzer *et al.* 2010, Laliberté *et al.* 2012). Changes in soil fertility during long-term soil and ecosystem development alter the functional composition of the vegetation, the amount and quality of resources entering the belowground subsystem (Richardson *et al.* 2004; Hayes *et al.* 2014; Zemunik *et al.* 2015) and the communities of organisms that constitute the soil food web and govern nutrient cycling, plant nutrition and growth (Williamson *et al.* 2005; Doblas-Miranda *et al.* 2008; Bokhorst *et al.* 2017).

At larger spatial scales, macroclimate is also well recognized as regulating pedogenesis, the nature of soil nutrient limitation and nutrient supply for plant growth (McGroddy *et al.* 2004; Huston 2012) and feedbacks between plants and the belowground subsystem (Defossez *et al.* 2011; De Long *et al.* 2015). However, large-scale studies exploring these effects are frequently confounded by differences in parent material under different climatic regimes, and there is a dearth of studies on how macroclimate and soil fertility interact in their effects on above- and belowground communities and ecosystem processes when parent material is held constant (but see Bokhorst *et al.* 2017). Insights can potentially be derived from studies that either explore interactions between parent material and climate (Kitayama & Aiba 2002), or interactions of soils of different ages and climate within a single parent material (Kitayama *et al.* 1997; Porder *et al.* 2007). For example, Porder and Chadwick (2009) showed, using a matrix of sites in Hawaii varying in soil age and climate, that ecosystem nutrient retention during pedogenesis is greatest when precipitation matches potential evapotranspiration. As such, the use of long-term chronosequences that encapsulate a wide range of soil fertilities across regional climate gradients has considerable potential for advancing understanding of how climatic constraints moderate the consequences of soil fertility for belowground community or ecosystem properties. However, to our knowledge such a test has never been performed.

The organisms in the belowground subsystem collectively comprise the soil food web, which contains three broadly-defined energy channels: bacterial-based, fungal-based and root-based (Moore & Hunt 1988; de Ruiter *et al.* 1995). The bacterial- and fungal-based channels influence plants indirectly by regulating the release of nutrients from labile and more recalcitrant organic matter, respectively, while the root-based channel involves mutualists (e.g., mycorrhizal fungi, nitrogen-fixing bacteria), pathogens and herbivores that interact directly with plants (Wardle *et al.* 2004a). The interactions of soil biota with plants regulate plant growth and vegetation change (De Deyn *et al.* 2003; Kardol *et al.* 2006) and ecosystem processes both above and below ground (Berendse 1998; Sackett *et al.* 2010). Despite the key role of the soil food web in terrestrial ecosystem functioning, we understand little about its response to large-scale variation in soil fertility outside of agricultural systems (Mulder *et al.* 2013). However, some insights have been revealed from retrogressive chronosequences in which large declines in soil fertility over time can lead to pronounced declines in densities of soil biota (Williamson *et al.* 2005; Doblas-Miranda *et al.* 2008; Peltzer *et al.* 2010) and increasing dominance by the fungal-based (versus the bacterial-based) energy channels (Wardle *et al.* 2004a; Williamson *et al.* 2005; Bokhorst *et al.* 2017). How these effects of retrogression (and thus declining soil fertility; i.e., bottom-up control) on the soil food web are moderated by climate remains unexplored, but addressing this would greatly aid understanding of how macroclimate drives ecosystem change. More generally, studying the interactive effects of soil fertility and climate is important because they represent the dominant abiotic factors controlling the functioning of terrestrial ecosystems worldwide.

A better understanding of the joint influences of climate and soil age on ecosystem development can be achieved through comparative analysis of multiple retrogressive chronosequences that are similar in parent material and mode of formation but differ strongly in macroclimate (Vitousek 2004). However, model systems that meet this strict requirement are very rare (but see Kitayama *et al.* 1997; Porder & Chadwick 2009). Here, we use a recently characterized soil age × climate gradient in south-western Australia consisting of four long-term coastal dune chronosequences (Turner *et al.* 2017) to determine how climate modulates changes in the soil food web that occur during long-term pedogenesis and ecosystem development. This question has not previously been explored in this way and can be addressed through our globally unique study system of comparable long term soil-aging chronosequences repeated across a strong climatic gradient. The northernmost and driest of the four chronosequences (Jurien Bay) is well characterized, and changes in soil and vegetation properties that occur during retrogression along this sequence (Laliberté *et al.* 2012; Hayes *et al.* 2014; Turner & Laliberté 2015) are consistent with those expected from the Walker and Syers (1976) model of long-term pedogenesis. For this study, we sampled an additional three long-term dune chronosequences from Jurien Bay to the

132 southern tip of south-western Australia that share the same mode of formation and relatively similar
133 parent material, but which differ strongly in climate (i.e. increasing rainfall and declining
134 temperature from north to south; Fig. 1; Turner *et al.* 2017). This network of chronosequences is
135 one of only two systems worldwide that enables the study of the joint influences of climate and soil
136 age on ecosystem development, and the only one in a Mediterranean climate region or within a
137 global biodiversity hotspot (Hopper & Gioia 2004; Turner & Laliberté 2015; Turner *et al.* 2017).
138 For each of the four sequences, we characterized five stages that encompass both the build-up
139 and retrogressive phases of ecosystem development. For each stage we quantified vegetation cover,
140 plant root mass, soil abiotic properties, and key components of the soil food web (i.e., major groups
141 of soil microbes, nematodes and microarthropods). These included groups of organisms in each of
142 the main energy channels (bacterial, fungal, root) as well as upper level predators where these
143 channels converge. Based on the rationale that soil food webs are often strongly bottom-up
144 controlled (Wardle and Yeates 1993, De Ruiter et al. 1995), we expected these food web
145 components to increase in biomass in the early stages of these chronosequences as organic matter
146 and N accumulate and root biomass increases, but decrease during late-stage retrogression as the
147 quality and quantity of resources entering the soil declines (thus yielding a humped response to
148 these components over time). However, we predicted that climate would moderate soil food web
149 development across the four chronosequences. Specifically, we tested two hypotheses. First, we
150 hypothesized that responses of the main groups of soil biota to pedogenesis would yield stronger
151 hump-backed relationships under higher precipitation. This is because alleviation of water
152 limitation should increase the responsiveness of the soil biota to soil fertility, and because
153 pedogenic processes that drive soil fertility and lead to retrogression are expected to occur faster
154 under level higher levels of precipitation (Peltzer *et al.* 2010; Huston 2012). Second, we
155 hypothesized that across each of the four chronosequences the bacterial energy channels would
156 dominate earlier than fungal channels (as fungal channels are more adapted to lower soil fertility
157 and more recalcitrant organic matter; Wardle *et al.* 2004a) and that there would be an increasingly
158 important role of the root channel (because plant biomass allocation to roots is greater under low
159 nutrient availability; Brouwer 1963; Grime 2001), with these changes being more pronounced for
160 the wetter sequences. For both hypotheses, we further expected that top-down control by predatory
161 organisms could be an additional driver of abundance of organisms at lower trophic levels of the
162 food web (Crowther *et al.* 2013; Kardol *et al.* 2016), especially during stages of ecosystem
163 development where soil fertility is high, i.e., in the absence of bottom-up control (Crowther *et al.*
164 2015). Such top-down control might be stronger under lower precipitation as higher-trophic level
165 organisms might be less sensitive to drought. Finally, we explored how food web structure was
166 differentially affected by soil fertility across contrasting rainfall regimes, and used structural

equation modeling (SEM) to determine how these effects were propagated through the soil food web.

MATERIAL AND METHODS

Study area and site selection

The study was conducted along each of four coastal dune chronosequences situated across south-western Australia (Fig. 1). The four dune chronosequences are positioned along a regional-scale climate gradient in which the northernmost chronosequence (Jurien Bay) is the warmest and driest and the southernmost one (Warren) is the wettest and coolest (Fig. 1). Because temperature and precipitation are very strongly correlated with each other across these four sequences (Fig. 1), we use annual water balance (i.e. precipitation – potential evapotranspiration) as our main climate variable, following Porder and Chadwick (2009). Water balance is arguably the single best and most ecologically important climatic variable in our study because it integrates both actual water supply (i.e. precipitation) as well as the driving force for water loss (i.e. potential evapotranspiration). Details on these four sequences are available in Appendix S1, Figure 1, and in Turner et al. (2017).

In each chronosequence, we first selected five chronosequence stages that represented increasing soil age and pedogenic development. In Jurien Bay, these five stages correspond to the same ones described and used by Hayes *et al.* (2014). Delineation of chronosequence stages and methods of site selection for the Jurien Bay chronosequence have been described elsewhere (Laliberté *et al.* 2014; Zemunik *et al.* 2015). Maps showing locations of each chronosequence stage are available in Turner et al. (2017). In Jurien Bay, we randomly selected four existing plots in each of the five chronosequence stages, from a network of permanent plots used in previous studies (Laliberté *et al.* 2014; Zemunik *et al.* 2015, 2016). For the other three chronosequences (Guilderton, Yalgorup, Warren; Fig. 1), we positioned four replicate sampling plots in each of the five chronosequence stages at random positions near soil profile pits (Turner *et al.* 2017), ensuring that replicate plots followed the same dune from which the profile pit was dug. Plots were 10 m × 10 m in size and positioned along a north-south axis. Replicate plots within each chronosequence stage were always positioned at least 50 m from each other, but ~100 m whenever possible. These plots were used for all measurements and sample collections.

196 **Leaf area index**

197 Leaf area index (LAI) was estimated in each plot over 10-26 September 2013, using a portable
198 plant canopy imager (CI-110, CID Bio-Science, Camas, WA, USA). We took four canopy images
199 per plot and sampling points within each plot were separated by 7 m. Images were taken with the
200 camera as close as possible to the ground surface to include low-lying vegetation. Images were
201 processed using the built-in software and LAI was calculated using the gap-fraction method (Bréda
202 2003). The four LAI measurements per plot were averaged prior to statistical analysis.

203 **Soil sampling and soil chemical analyses**

204 To quantify changes in soil chemical properties, we sampled surface soils (0-10 cm depth) in each
205 plot, 10-26 September 2013. We collected four soil samples using a 50-mm diameter sand auger at
206 the same positions where LAI measurements were made. Those four soil samples were bulked and
207 homogenized at the plot level and two fresh sub-samples were taken from these for characterization
208 of microbial and nematode communities, respectively. These sub-samples were stored in a portable
209 refrigerator and maintained at 10 °C until further processing. The remaining sample material was
210 air-dried for soil chemical analyses. Total carbon (C), organic C, carbonate content, total N, total P,
211 resin-extractable P, pH, bulk density, and exchangeable cations were measured as described in
212 Turner and Laliberté (2015). In each plot, we also sampled four 0-10 cm deep, 10-cm diameter
213 cores using PVC pipe for extraction of soil microarthropods. Each PVC pipe was carefully inserted
214 into the soil and retrieved with a trowel. Cores were capped and immediately transferred in a cooler
215 for transportation from field sites.

216 **Microbial analyses**

217 Community compositional data for soil microbes was obtained for a 1 g subsample of each soil
218 sample, by measuring phospholipid fatty acids (PLFAs) using the method of Bligh and Dyer
219 (1959), as modified by White *et al.* (1979); different PLFAs represent different subsets of the soil
220 microflora. Details of microbial analyses are available in Appendix S1. Microbial biomass data are
221 reported both per g dry soil weight and per g organic C. We do not report results on a soil volume
222 (or areal) basis because differences in soil bulk density among chronosequences and stages are
223 small (Turner & Laliberté 2015; Turner *et al.* 2017) and analyses on a soil volume basis showed
224 qualitatively similar patterns to those analyzed on a dry soil weight basis (results not shown).

225 **Nematodes**

226 Nematodes were extracted from a 150 g sub-sample of each soil sample, using a sugar flotation
227 method (Jenkins 1964), for determinations of abundance and biomass. Nematodes were heat-killed
228 and fixed using 4% (v/v) formaldehyde. At least 150 randomly selected individuals in each sample
229 were identified to family level. Nematodes were then allocated to five trophic groups based on
230 Yeates *et al.* (1993). Details on classification into feeding groups and biomass estimation are
231 available in Appendix S1.

232 **Microarthropods**

233 Within 72 hours after sampling, PCV cores containing soil samples were transferred into Berlese
234 funnels for microarthropod extraction (Southwood & Henderson 2000) over a 72-hr period.
235 Microarthropods were identified and counted; this data was used for determining abundance and
236 biomass. Details of the classification into different feeding groups (Table S1), and biomass
237 estimation, are available in Appendix S1. Count data from the four core samples per plot were
238 pooled together for the purposes of analysis.

239 **Roots**

240 Once all microarthropods were extracted, we removed all roots from soil cores, bulked them at the
241 plot level, carefully washed them over a 1-mm sieve, and oven-dried them at 60°C for four days
242 before weighing.

243 **Statistical analyses**

244 Detailed explanation of the statistical analyses is presented in Appendix S1. Briefly, all response
245 variables were analyzed using linear mixed-effect models. We treated chronosequence stage as a
246 fixed effect, with random intercepts per chronosequence. To evaluate whether responses of
247 individual variables varied across stages among chronosequences, we compared this first model to
248 a second one that also considered random intercepts per stage nested within chronosequence, using
249 likelihood ratio tests (Pinheiro & Bates 2000). We tested for differences among stages using *post*
250 *hoc* Tukey tests (Hothorn *et al.* 2008). These analyses were conducted in R (R Development Core
251 Team 2016) using the 'nlme' (Pinheiro *et al.* 2015) and 'multcomp' (Hothorn *et al.* 2008)
252 packages.

253 We used generalized multilevel path models (Shipley 2009) to test multivariate causal
254 hypotheses linking climate, pedogenesis, and their joint influence on soil food webs.

Chronosequence stage was treated as a ranked variable. We used water balance (i.e., mean annual precipitation minus mean annual potential evapotranspiration) as a proxy for macroclimatic variation across chronosequences. Food web components were expressed on a biomass per dry soil weight basis. Most variables were log-transformed to linearize relationships. We used second-order polynomials of 'chronosequence stage' to model humped-back relationships (Grace *et al.* 2007). All variables were centered on their means to facilitate interpretation of path coefficients and to avoid multicollinearity problems due to the inclusion of interactions and polynomials (Aiken & West 1991). Path models were fitted in R (R Development Core Team 2016) using the 'piecewiseSEM' package (Lefcheck 2016), while individual models were fitted using the 'nlme' package (Pinheiro *et al.* 2015).

RESULTS

Soil organic matter and vegetation

Changes in soil organic matter during long-term ecosystem development varied among chronosequences (Table S2, Fig. 2a), but organic matter was lowest at the youngest stage for all sequences and highest at the intermediate stages for all sequences except Yalgorup (Fig. 1a). Changes in LAI also varied among chronosequences (Table S2, Fig. 2b); there were no differences in LAI among stages in the driest chronosequence (Jurien Bay), and a progressively stronger humped-back pattern with increasing rainfall for the other three (Fig. 2b). On average, leaf area index increased from drier to wetter climates (Fig. 2b). There were consistent increases in root weight with increasing soil age across chronosequences (Table S2, Fig. 2c), as indicated by a non-significant chronosequence × stage interaction but significant overall differences among stages (Table S2).

Microorganisms

Changes in bacterial and fungal biomass, and the ratio of fungal to fungal plus bacterial biomass during ecosystem development, varied among chronosequences. Fungal biomass per g soil was always lowest in the youngest stage, but never differed significantly among the other four stages, although the relationship was most hump-shaped for the wettest sequence which also showed significantly ($P \leq 0.004$, following *post hoc* tests) higher fungal biomass than the two driest ones (Fig. 3a). When expressed per g soil C, fungal biomass was much higher for the wettest sequence than for the other three sequences, but with the exception of Guilderton (which had a lower biomass in stage 1 than in stages 2 and 4), it did not change during ecosystem development (Fig. S1a).

Across the four chronosequences, bacterial biomass per g soil generally showed a hump-shaped relationship with peak biomass at intermediate stage, but the hump-shape was most pronounced for the two driest sequences (Fig. 3b). When expressed per g soil C, the hump-shaped relationships disappeared and instead bacterial biomass decreased with soil aging for Guilderton and Yalgorup (Fig. S1b). Actinomycetes, and branched and cyclic bacterial PLFAs, showed similar responses to total bacteria, both when expressed per g soil and per g soil C (Table S2; data not presented).

The ratio of fungal to bacterial biomass showed a U-shaped relationship with stage for the driest chronosequence and increased at later stages for the second driest sequence, but was unresponsive for the other two sequences (Fig. 3c).

Nematodes

Responses of all nematode groups except omnivores to ecosystem development were consistent across the four chronosequences (Table S2). Fungal-feeding nematodes increased with soil age when expressed per g soil (Fig. 4a), but showed a U-shaped response when expressed per g soil C (Fig. S2a). Bacterial-feeding nematodes were greatest at intermediate stages when expressed per g soil (Fig. 4b), and decreased with soil age when expressed per g soil C (Fig. S2b). The ratio of fungal-feeding to fungal-feeding plus bacterial-feeding nematodes was significantly greater at the oldest stage than at the other four stages (Fig. 4c). Across chronosequences, herbivorous (plant-feeding + root-associated) nematodes were highest at an intermediate stage when expressed per g soil (Fig. 4d), and at the first three stages when expressed per g plant root (Fig. S3c). For omnivorous nematodes per g soil, patterns varied across chronosequences (Table S2, Fig. 4e) with significant humped-back patterns only for the two driest sequences. There were no significant differences in the biomass of carnivorous nematodes across chronosequences or stages (Table S2; data not presented).

Microarthropods

For all three groups of microarthropods (fungal-feeding Collembola, fungal-feeding mites and predatory mites), responses to soil aging differed among chronosequences (Table S2, Fig. 5) when expressed per g soil. Collembola generally showed no significant responses to soil aging, except for Yalgorup (second-wettest sequence) where biomass declined from the first to the second stage (Fig. 5a). Fungal-feeding mites increased in abundance with soil aging in the second-driest and wettest chronosequence, but not in the other two (Fig. 5b). Biomass of predatory mites increased with soil age in the second-driest sequence, but did not differ among stages in the other three sequences (Fig. 5c). When expressed per g soil C, biomass of fungal-feeding mites was lowest in intermediate

318 stages in the two driest chronosequences, but did not vary among stages in the two wettest
319 sequences (Fig. S3); it was also significantly higher (Table S2; $P = 0.001$, following *post hoc* tests)
320 in the wettest sequence. Meanwhile Collembola biomass per g soil C did not vary across
321 chronosequence stages (Table S2; data not presented).

322 **Structural equation modeling**

323 Our multivariate causal model linking climate, long-term soil development, and soil food webs was
324 supported by the data ($\chi^2 = 90.7$, df = 74, $P = 0.091$; Fig. 6). Specifically, it showed that soil aging
325 had large effects on basal resources (i.e., soil organic C and root biomass) while climate did not
326 (Fig. 6). Of the basal resources, root biomass increased with soil age while soil organic C showed a
327 hump-shaped relationship (as revealed by the importance of including 'stage' as a quadratic term;
328 Fig. 6). These basal resources in turn had strong direct positive effects on biomass of first-order
329 consumers (i.e., bacteria, fungi and herbivorous nematodes; Fig. 6). However, effects of soil aging
330 on first-order consumers were not only manifested indirectly via the quantity of these basal
331 resources, but also directly. These direct responses of consumers to stage were hump-shaped and
332 could reflect differences in resource quality (Fig. 6). In addition, biomasses of bacteria and fungi
333 were correlated with each other even after taking into account their respective common drivers
334 (Fig. 6), suggesting that the two groups may be responding similarly to variables not included in the
335 model.

336 Biomasses of second- and third-order consumers, except for fungal-feeding mites and
337 Collembola, were directly influenced by their prey within each of the different energy channels
338 (Fig. 6). Bacterial-feeding nematodes primarily increased with bacterial biomass, and fungal-
339 feeding nematodes primarily increased with fungal biomass (Fig. 6). Finally, biomass of
340 omnivorous and carnivorous nematodes increased with that of bacterial-feeding nematodes, while
341 biomass of predatory mites increased with that of fungal-feeding mites (Fig. 6).

342 A revised model that included soil N and P concentrations (Fig. S4) was qualitatively similar,
343 but adding these variables as potential indicators of resource quality did not assist interpretation
344 because direct paths between stage and basal resources (i.e. soil organic C, root biomass) and basal
345 consumers (i.e. bacteria, fungi, and root-feeding nematodes) remained significant in the model (Fig.
346 S4).

347 **DISCUSSION**

348 Our study of belowground food webs across four long-term retrogressive soil chronosequences
349 along a regional climate gradient highlights the overarching importance of soil fertility in regulating

the bottom-up control of food webs, relative to climate. Basal consumers showed hump-shaped responses to soil aging, which were propagated to higher-order consumers. Our study provides further support for a general shift from dominance by the bacterial to the fungal energy channel with increasing soil age (Bokhorst *et al.* 2017).

We found partial support for our first hypothesis that the basal resources supporting the soil food web, as well as the different food web components themselves, would show hump-shaped responses to soil aging during long-term ecosystem development. For basal resources, hump-shaped responses were observed for soil organic matter, but not for root biomass which increased steadily as soils aged. This increase in root biomass likely reflects greater plant allocation to roots as soil nutrient availability declines (Brouwer 1963; Grime 2001), given that soil aging across these chronosequences is associated with declining soil fertility (Turner & Laliberté 2015; Turner *et al.* 2017). Basal consumers (i.e. bacteria, fungi, and herbivorous nematodes) often showed hump-shaped relationships with soil aging. However, the higher-order consumers did not, with the exception of omnivorous nematodes in the two driest chronosequences. This could be because prey abundance does not explain all of the variation in higher-order consumers; other sources of variation can 'mask' the hump-shaped signal of prey abundance. Instead, our multivariate causal model showed that higher-order consumers (and, to a lesser extent, basal consumers) were controlled primarily by the abundance of their prey, suggesting primarily an indirect effect of soil age. Overall, our results are consistent with soil aging having strong direct effects on basal resources, and with these effects being propagated through the soil food web (Williamson *et al.* 2005; Doblas-Miranda *et al.* 2008; Bokhorst *et al.* 2017).

Hump-shaped responses of bacteria and fungi to soil aging were primarily driven by changes in soil organic matter quantity, rather than quality. Indeed, once bacterial and fungal biomass was expressed on a soil organic C basis (as opposed to on a soil weight basis) to account for potential differences in resource quantity, the hump-shaped responses of these organisms to soil aging largely disappeared. However, even though bacteria and fungi were mostly driven by soil organic matter quantity, our multivariate causal model showed additional direct effects of soil aging, which could be reflective of changes in resource quality. Further, hump-shaped response of herbivorous nematodes (per g soil) to soil aging, which are in line with previous studies (Doblas-Miranda *et al.* 2008), was reflective of both changes in resource quantity (i.e. root biomass increasing from stage 1 to 3) and resource quality (i.e. lower herbivorous nematode biomass per unit root mass in stages 4 and 5). Although we did not measure root quality in our study, foliar and fine root nutrient concentrations are generally correlated (Freschet *et al.* 2010; Reich 2014), and previous studies along the Jurien Bay chronosequence have shown strong declines in foliar nutrients during

retrogression (Hayes *et al.* 2014). Therefore, declines in root nutrient concentrations might explain the decline in herbivorous nematodes from stages 3 to 5, despite higher root mass in these soils.

We found equivocal support for our hypothesis that macroclimate moderates soil food web responses to soil aging. On one hand, individual analyses of responses of soil microbiota (bacteria and fungi) and microarthropods often showed variable responses to soil aging across the different chronosequences. For example, hump-shaped responses of leaf area index (which influences the amount of leaf litter entering the soil) and fungal biomass to soil aging became more pronounced in wetter climates which was in line with our hypothesis; the changes in fungal biomass are likely to be reflective of the importance of bottom-up regulation for fungi (Wardle & Yeates 1993; de Ruiter *et al.* 1995). On the other hand, responses to soil aging of root biomass, as well as biomass of all nematode groups except omnivores, were not influenced by climate and were consistent across the four chronosequences. In addition, our multivariate causal model showed that soil aging, but not macroclimate, had strong effects on basal resources, which were propagated through the food webs. Overall, our structural equation modelling results show that while climate moderated responses of some food web components in the manner predicted by our hypothesis, effects of climate were frequently overridden by those of soil aging.

The relatively modest effect of climate, and the consistent responses of root biomass and most nematode groups to soil aging, was unexpected given the large differences in macroclimate across the four dune chronosequences (i.e. annual water balance ranged from 900 mm deficit in Jurien Bay to 52 mm excess in Warren) as well as the known importance of precipitation as a driver of nematode communities at both local (Kardol *et al.* 2010) and regional (Chen *et al.* 2015) scales. This suggests that nutrient limitation during pedogenesis has stronger effects on soil food webs than do large differences in climate. However, the importance of soil fertility in our study might in part reflect the fact that differences in soil nutrients across each of these four long-term chronosequences are relatively large. For example, the ~60-fold range in total soil [P] in Jurien Bay is comparable to that found across all ecosystems worldwide, making it one of the strongest natural soil fertility gradients characterized to date (Turner & Laliberté 2015).

We found partial evidence for our second hypothesis predicting a shift from the bacterial to the fungal energy channel with soil aging; notably the ratio of fungal-feeding nematodes to fungal + bacterial-feeding nematodes was consistently greatest in the oldest soils. Our finding that the response of this ratio to soil aging was invariant across the four chronosequences is, however, contrary to our hypothesis that it would be more pronounced in wetter climates. The consistency in this response suggests that the greater relative importance of fungal (versus bacterial) energy channel with declining soil fertility (Wardle *et al.* 2004a; Williamson *et al.* 2005; Doblas-Miranda *et al.* 2008; Bokhorst *et al.* 2017) may be a widespread pattern across contrasting climates.

However, contrary to nematodes, increases in fungal biomass relative to bacterial biomass with soil aging were only observed for one of the four chronosequences (Guilderton), which may be due to differential importance of top-down regulation of fungal and bacterial biomass by their consumers (Wardle & Yeates 1993; de Ruiter *et al.* 1995; Moore *et al.* 2003). But, contrary to our expectation, these data did not indicate that the strength of top-down control increased in drier climates, further supporting our finding that bottom-up control through nutrient limitation is the main driver of soil food web development during long-term ecosystem development. Further, our hypothesis predicting that the relative importance of the root energy channel for the soil food web would increase with soil aging was not supported. Indeed, even though root biomass showed a consistent increase with soil aging across all four chronosequences, the response of herbivorous nematodes to soil aging was hump-shaped, suggesting that declines in root quality during retrogression diminish the importance of the root energy channel. The importance of root quality in driving densities of root feeding organisms has also been suggested for shorter term successional sequences (Holtkamp *et al.* 2008).

By sampling a regional soil age × climate gradient, we were able to determine how macroclimate moderates soil food web responses to long-term soil aging during both the build-up and retrogressive phases of ecosystem development. Contrary to our hypotheses, we found that climate had relatively small and often variable effects on soil food webs compared to the large effects of soil aging. In fact, our results showed consistent responses to soil aging for several food web components (notably nematodes) across the four chronosequences, despite important differences in climate. This result was unexpected given the strong role of climate in pedogenesis (Porder & Chadwick 2009; Huston 2012). Our use of structural equation modeling provided additional insights about the cascading effects of soil aging on soil food webs through effects on basal resources, highlighting the importance of bottom-up controls within the different energy channels. We note, however, that for quantitative insights on flux rates across trophic levels of the soil food web other methods would be needed (e.g., isotopic tracers) (Rousk 2016). In conclusion, our study highlights some consistencies regarding the role of soil aging and associated nutrient limitation in regulating soil food webs across contrasting climatic conditions, and in how changes in basal resources with soil age are propagated to higher trophic levels (Wardle *et al.* 2004a; Williamson *et al.* 2005; Doblas-Miranda *et al.* 2008). Our finding that effects of nutrient limitation on belowground food webs overwhelm those of climate suggests that global environmental changes that directly or indirectly affect soil nutrient availability should have stronger impacts on belowground communities than changes in climate. These insights are important in our thinking about how global changes impact on terrestrial ecosystems.

ACKNOWLEDGEMENTS

We thank Oleksandr Holovachov for advice on nematode identifications, Peter Langlands for microarthropod sorting and counting, and the Department of Parks and Wildlife of Western Australia for their collaboration with field work. Funding was provided by a Discovery Project from the Australian Research Council (DP130100016). DAW was supported by a Wallenberg Scholars award.

DATE ACCESSIBILITY

The data supporting the results are available from the Dryad Digital Repository (doi:10.5061/dryad.6cs14).

REFERENCES

Aiken, L.S. & West, S.G. (1991). Multiple Regression: Testing and Interpreting Interactions. Sage Publications, Newbury Park, USA

Berendse, F. (1998). Effects of dominant plant species on soils during succession in nutrient-poor ecosystems. *Biogeochemistry*, 42, 73–88

Bligh, E.G. & Dyer, W.J. (1959). A rapid method of total lipid extraction and purification. *Can. J. Biochem. Physiol.*, 37, 911–917

Bokhorst, S., Kardol, P., Bellingham, P.J., Kooyman, R.M., Richardson, S.J., Schmidt, S., et al. (2017). Response of communities of soil organisms and plants to soil aging at two contrasting long-term chronosequences. *Soil Biol. Biochem.*, 106,, 69–79

Bréda, N.J.J. (2003). Ground-based measurements of leaf area index: a review of methods, instruments and current controversies. *J. Exp. Bot.*, 54, 2403–2417

Brouwer, R. (1963). Some aspect of the equilibrium between overground and underground plant parts. *Jaarb. Van Het Inst. Voor Biol. En Scheikd. Onderz. Aan Landbouwgewassen*, 31–39

Chen, D., Cheng, J., Chu, P., Hu, S., Xie, Y., Tuvshintogtokh, I., et al. (2015). Regional-scale patterns of soil microbes and nematodes across grasslands on the Mongolian plateau: relationships with climate, soil, and plants. *Ecography*, 38, 622–631

Crowther, T.W., Stanton, D.W.G., Thomas, S.M., A'Bear, A.D., Hiscox, J., Jones, T.H., et al. (2013). Top-down control of soil fungal community composition by a globally distributed keystone consumer. *Ecology*, 94, 2518–2528

Crowther, T.W., Thomas, S.M., Maynard, D.S., Baldrian, P., Covey, K., Frey, S.D., et al. (2015). Biotic interactions mediate soil microbial feedbacks to climate change. *Proc. Natl. Acad. Sci.*, 112, 7033–7038

De Deyn, G.B., Raaijmakers, C.E., Rik Zoomer, H., Berg, M.P., de Ruiter, P.C., Verhoef, H.A., et al. (2003). Soil invertebrate fauna enhances grassland succession and diversity. *Nature*, 422, 711–713

De Long, J.R., Kardol, P., Sundqvist, M.K., Veen, G.F. (Ciska) & Wardle, D.A. (2015). Plant growth response to direct and indirect temperature effects varies by vegetation type and elevation in a subarctic tundra. *Oikos*, 124, 772–783

Defossez, E., Courbaud, B., Marcais, B., Thuiller, W., Granda, E. & Kunstler, G. (2011). Do interactions between plant and soil biota change with elevation? A study on Fagus sylvatica. *Biol. Lett.*, rsbl20110236

Doblas-Miranda, E., Wardle, D.A., Peltzer, D.A. & Yeates, G.W. (2008). Changes in the community structure and diversity of soil invertebrates across the Franz Josef Glacier chronosequence. *Soil Biol. Biochem.*, 40, 1069–1081

Freschet, G.T., Cornelissen, J.H.C., Van Logtestijn, R.S.P. & Aerts, R. (2010). Evidence of the "plant economics spectrum" in a subarctic flora. *J. Ecol.*, 98, 362–373

Grace, J.B., Anderson, T.M., Smith, M.D., Seabloom, E., Andelman, S.J., Meche, G., et al. (2007). Does species diversity limit productivity in natural grassland communities? *Ecol. Lett.*, 10, 680–689

Grime, J.P. (2001). Plant Strategies, Vegetation Processes and Ecosystem Properties. 2nd edn. Wiley, New York, USA

Hayes, P., Turner, B.L., Lambers, H. & Laliberté, E. (2014). Foliar nutrient concentrations and resorption efficiency in plants of contrasting nutrient-acquisition strategies along a 2-million-year dune chronosequence. *J. Ecol.*, 102, 396–410

Holtkamp, R., Kardol, P., van der Wal, A., Dekker, S.C., van der Putten, W.H. & de Ruiter, P.C. (2008). Soil food web structure during ecosystem development after land abandonment. *Appl. Soil Ecol.*, 39, 23–34

Hopper, S.D. & Gioia, P. (2004). The Southwest Australian Floristic Region: evolution and conservation of a global hot spot of biodiversity. *Annu. Rev. Ecol. Evol. Syst.*, 35, 623–650

Hothorn, T., Bretz, F. & Westfall, P. (2008). Simultaneous inference in general parametric models. *Biom. J.*, 50, 346–363

Huston, M.A. (2012). Precipitation, soils, NPP, and biodiversity: resurrection of Albrecht's curve. *Ecol. Monogr.*, 82, 277–296

Jenkins, W.R. (1964). A rapid centrifugal-flotation technique for separating nematodes from soil. *Plant Dis. Rep.*, 48, 692

Kardol, P., Cregger, M.A., Campany, C.E. & Classen, A.T. (2010). Soil ecosystem functioning under climate change: plant species and community effects. *Ecology*, 91, 767–781

Kardol, P., Martijn Bezemer, T. & Van Der Putten, W.H. (2006). Temporal variation in plant–soil feedback controls succession. *Ecol. Lett.*, 9, 1080–1088

Kardol, P., Spitzer, C.M., Gundale, M.J., Nilsson, M.-C. & Wardle, D.A. (2016). Trophic cascades in the bryosphere: the impact of global change factors on top-down control of cyanobacterial N_2-fixation. *Ecol. Lett.*, 19, 967–976

Kitayama, K. & Aiba, S.-I. (2002). Ecosystem structure and productivity of tropical rain forests along altitudinal gradients with contrasting soil phosphorus pools on Mount Kinabalu, Borneo. *J. Ecol.*, 90, 37–51

Kitayama, K., Schuur, E.A.G., Drake, D.R. & Mueller-Dombois, D. (1997). Fate of a wet montane forest during soil ageing in Hawaii. *J. Ecol.*, 85, 669–679

Laliberté, E., Turner, B.L., Costes, T., Pearse, S.J., Wyrwoll, K.-H., Zemunik, G., et al. (2012). Experimental assessment of nutrient limitation along a 2-million year dune chronosequence in the south-western Australia biodiversity hotspot. *J. Ecol.*, 100, 631–642

Laliberté, E., Zemunik, G. & Turner, B.L. (2014). Environmental filtering explains variation in plant diversity along resource gradients. *Science*, 345, 1602–1605

Lefcheck, J.S. (2016). piecewiseSEM: Piecewise structural equation modeling in R for ecology, evolution, and systematics. *Methods Ecol. Evol.*, 7, 573–579

McGroddy, M.E., Daufresne, T. & Hedin, L.O. (2004). Scaling of C:N:P stoichiometry in forests worldwide: implications of terrestrial Redfield-type ratios. *Ecology*, 85, 2390–2401

Moore, J.C. & Hunt, H.W. (1988). Resource compartmentation and the stability of real ecosystems. *Nature*, 333, 261–263

Moore, J.C., McCann, K., Setälä, H., Ruiter, D. & C, P. (2003). Top-down is bottom-up: does predation in the rhizosphere regulate aboveground dynamics? *Ecology*, 84, 846–857

Mulder, C., Ahrestani, F.S., Bahn, M., Bohan, D.A., Bonkowski, M., Griffiths, B.S., et al. (2013). Connecting the Green and Brown Worlds. *Adv. Ecol. Res.*, Ecological Networks in an Agricultural World, 49, 69–175

Peltzer, D.A., Wardle, D.A., Allison, V.J., Baisden, W.T., Bardgett, R.D., Chadwick, O.A., et al. (2010). Understanding ecosystem retrogression. *Ecol. Monogr.*, 80, 509–529

Pinheiro, J., Bates, D., DebRoy, S., Sarkar, D. & R Development Core Team. (2015). nlme: Linear and Nonlinear Mixed Effects Models. The Comprehensive R Archive Network (CRAN), Vienna, Austria

Pinheiro, J.C. & Bates, D.M. (2000). Mixed-Effects Models in S and S-PLUS. Springer, New York, USA

Porder, S. & Chadwick, O.A. (2009). Climate and soil-age constraints on nutrient uplift and retention by plants. *Ecology*, 90, 623–636

556 Porder, S., Hilley, G.E. & Chadwick, O.A. (2007). Chemical weathering, mass loss, and dust inputs
557 across a climate by time matrix in the Hawaiian Islands. Earth Planet. *Sci. Lett.*, 258, 414–427
558 van der Putten, W.H., Bardgett, R.D., Bever, J.D., Bezemer, T.M., Casper, B.B., Fukami, T., et al.
559 (2013). Plant–soil feedbacks: the past, the present and future challenges. *J. Ecol.*, 101, 265–276
560 R Development Core Team. (2016). R: A Language and Environment for Statistical Computing. R
561 Foundation for Statistical Computing, Vienna, Austria
562 Reich, P.B. (2014). The world-wide "fast–slow" plant economics spectrum: a traits manifesto. *J.*
563 *Ecol.*, 102, 275–301
564 Richardson, S.J., Peltzer, D.A., Allen, R.B., McGlone, M.S. & Parfitt, R.L. (2004). Rapid
565 development of phosphorus limitation in temperate rainforest along the Franz Josef soil
566 chronosequence. *Oecologia*, 139, 267–276
567 Rousk, J. (2016). Biomass or growth? How to measure soil food webs to understand structure and
568 function. *Soil Biol. Biochem.*, 102, 45–47
569 de Ruiter, P.C., Neutel, A.-M. & Moore, J.C. (1995). Energetics, patterns of interaction strengths,
570 and stability in real ecosystems. *Science*, 269, 1257–1260
571 Sackett, T.E., Classen, A.T. & Sanders, N.J. (2010). Linking soil food web structure to above- and
572 belowground ecosystem processes: a meta-analysis. *Oikos*, 119, 1984–1992
573 Shipley, B. (2009). Confirmatory path analysis in a generalized multilevel context. *Ecology*, 90,
574 363–368
575 Southwood, T.R.E. & Henderson, P.A. (2000). Ecological Methods. 3rd edition. London, UK
576 Turner, B.L., Hayes, P.E. & Laliberté, E. (2017). A climosequence of chronosequences in
577 southwestern Australia. *bioRxiv*, 113308
578 Turner, B.L. & Laliberté, E. (2015). Soil development and nutrient availability along a 2 million-
579 year coastal dune chronosequence under species-rich mediterranean shrubland in southwestern
580 Australia. *Ecosystems*, 18, 287–309
581 Vitousek, P.M. (2004). Nutrient cycling and limitation: Hawai'i as a model system. Princeton
582 University Press
583 Walker, T.W. & Syers, J.K. (1976). The fate of phosphorus during pedogenesis. *Geoderma*, 15, 1–
584 19
585 Wardle, D.A., Bardgett, R.D., Klironomos, J.N., Setälä, H., Van der Putten, W.H. & Wall, D.H.
586 (2004a). Ecological linkages between aboveground and belowground biota. *Science*, 304, 1629–
587 1633
588 Wardle, D.A., Walker, L.R. & Bardgett, R.D. (2004b). Ecosystem properties and forest decline in
589 contrasting long-term chronosequences. *Science*, 305, 509–513

Wardle, D.A. & Yeates, G.W. (1993). The dual importance of competition and predation as regulatory forces in terrestrial ecosystems: evidence from decomposer food-webs. *Oecologia*, 93, 303–306

White, D.C., Davis, W.M., Nickels, J.S., King, J.D. & Bobbie, R.J. (1979). Determination of the sedimentary microbial biomass by extractible lipid phosphate. *Oecologia*, 40, 51–62

Williamson, W.M., Wardle, D.A. & Yeates, G.W. (2005). Changes in soil microbial and nematode communities during ecosystem decline across a long-term chronosequence. *Soil Biol. Biochem.*, 37, 1289–1301

Yeates, G.W., Bongers, T., De Goede, R.G.M., Freckman, D.W. & Georgieva, S.S. (1993). Feeding habits in soil nematode families and genera—an outline for soil ecologists. *J. Nematol.*, 25, 315–331

Zemunik, G., Turner, B.L., Lambers, H. & Laliberté, E. (2015). Diversity of plant nutrient-acquisition strategies increases during long-term ecosystem development. *Nat. Plants*, 1, 15050

Zemunik, G., Turner, B.L., Lambers, H. & Laliberté, E. (2016). Increasing plant species diversity and extreme species turnover accompany declining soil fertility along a long-term chronosequence in a biodiversity hotspot. *J. Ecol.*, 104, 792–805

SUPPORTING INFORMATION

Additional Supporting Information may be downloaded via the online version of this article at Wiley Online Library (www.ecologyletters.com).

As a service to our authors and readers, this journal provides supporting information supplied by the authors. Such materials are peer-reviewed and may be re-organized for online delivery, but are not copy-edited or typeset. Technical support issues arising from supporting information (other than missing files) should be addressed to the authors.

Figure legends

Figure 1. Climatic data and photos showing changes in vegetation during ecosystem development for each of the four chronosequences. Age estimations are based on soil maps, soil characteristics and degree of pedogenesis (ref). Climate data are from Turner et al. (2017). Photo credits: P. Kardol, E. Laliberté, F. Teste, B. Turner and G. Zemunik. PET = potential evapotranspiration.

Figure 2. (**a**) Soil organic carbon, (**b**) leaf area index (LAI), and (**c**) root weight (0-10 cm depth). Bar heights represent means (n = 4) and error bars are 95% confidence intervals from linear mixed-effect models. Different letters indicate statistically significant differences ($P \leq 0.05$) among stages

within each chronosequence. Linear mixed effects model outputs for these data are given in Table S2. Root weight data are averaged across all sequences because responses to chronosequence stage did not differ among sequences.

Figure 3. (**a**) Fungal biomass, (**b**) bacterial biomass, and (**c**) the ratio (fungal biomass)/(fungal + bacterial biomass) along the four chronosequences. Microbial biomass was calculated from PLFA data and reported on a dry soil weight basis. Bar heights represent means (n = 4) and error bars are 95% confidence intervals from linear mixed-effect models. Different letters indicate statistically significant differences ($P \leq 0.05$) among stages within each chronosequence. Linear mixed effects model outputs for these data are given in Table S2.

Figure 4. Nematode biomass along the four chronosequences categorised into different feeding groups: (**a**) fungal feeders, (**b**) bacterial feeders, (**c**) ratio of fungal-feeders to (fungal feeders + bacterial-feeders), (**d**) plant feeders and root associates, and (**e**) omnivores. Bar heights represent means (n = 4) and error bars are 95% confidence intervals from linear mixed-effect models. Different letters indicate statistically significant differences ($P \leq 0.05$) among stages within each chronosequence. Linear mixed effects model outputs for these data are given in Table S2. For panels (a) to (d) data are averaged across all sequences because responses to chronosequence stage did not differ among sequences.

Figure 5. Microarthropod biomass along the four chronosequences: (**a**) fungal-feeding mites, (**b**) predatory mites, and (**c**) fungal-feeding Collembola. Bar heights represent means (n = 4) and error bars are 95% confidence intervals from linear mixed-effect models. Different letters indicate statistically significant differences ($P \leq 0.05$) among stages within each chronosequence. Linear mixed effects model outputs for these data are given in Table S2.

Figure 6. Generalized multilevel path model showing the direct and indirect pathways through which long-term soil and ecosystem development and climate together influence soil food webs. Here, soil and ecosystem development is represented by chronosequence stage, while climate is represented by the water balance (= rainfall - potential evapotranspiration). The model was supported by the data (χ^2 = 90.7, df = 74, P = 0.091). Arrows represent the flow of causality. Double-headed arrows represent correlated errors, with no hypothesized directed causal relationship. Solid arrows represent statistically significant ($P \leq 0.05$) relationships, while dashed grey arrows represent non-significant relationships. Arrow width is proportional to the standardized path coefficients. Unstandardized path coefficients associated with each solid arrow are shown.

660 Stage^2 is a second-order polynomial used to model humped-back responses to ecosystem
661 development. TL = trophic level; Carniv. = carnivorous; Omniv. = omnivorous. *$P \leq 0.05$, **$P \leq$
662 0.01, ***$P \leq 0.001$, ****$P \leq 0.0001$.

Figure 1

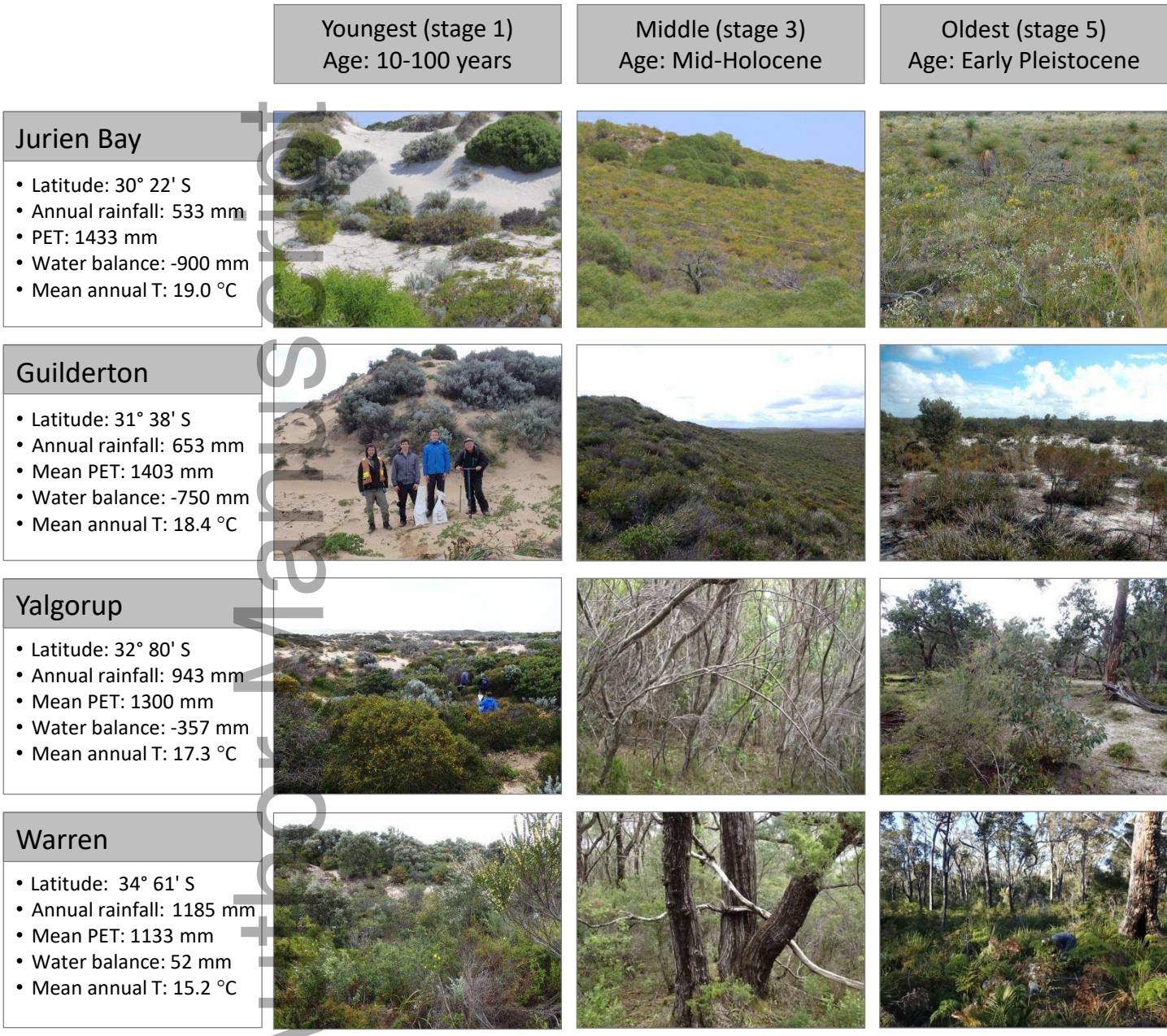

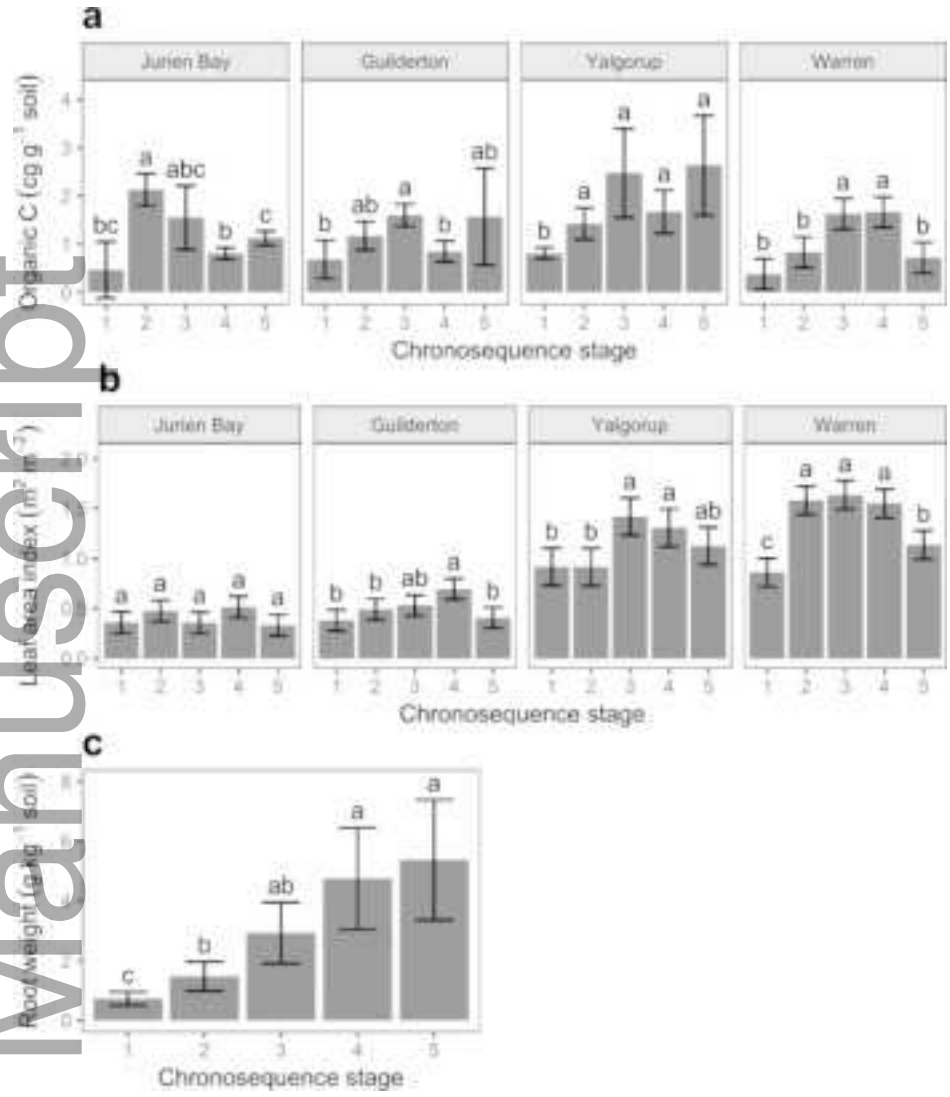

ele_12823_f2.tif

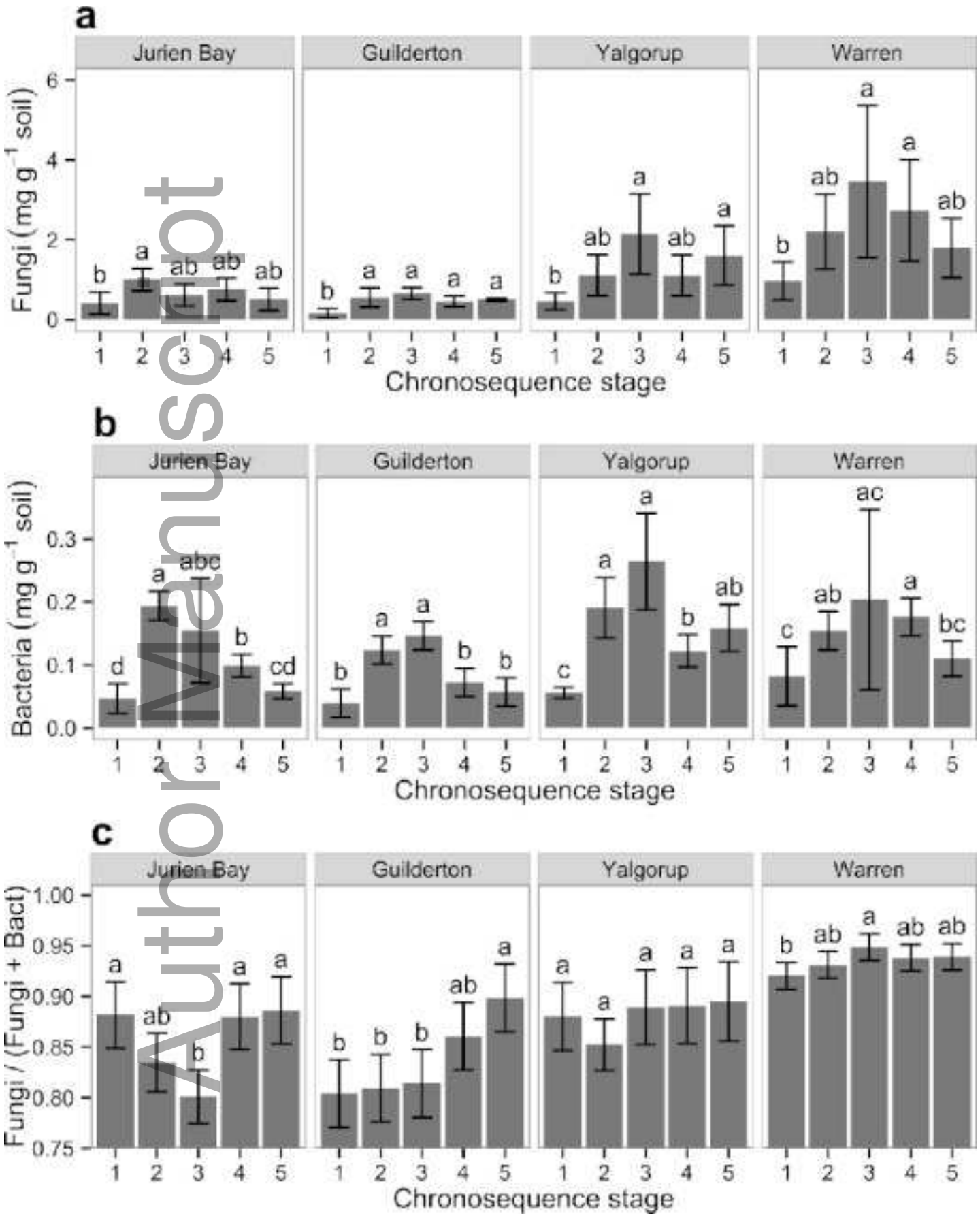

ele_12823_f3.tif

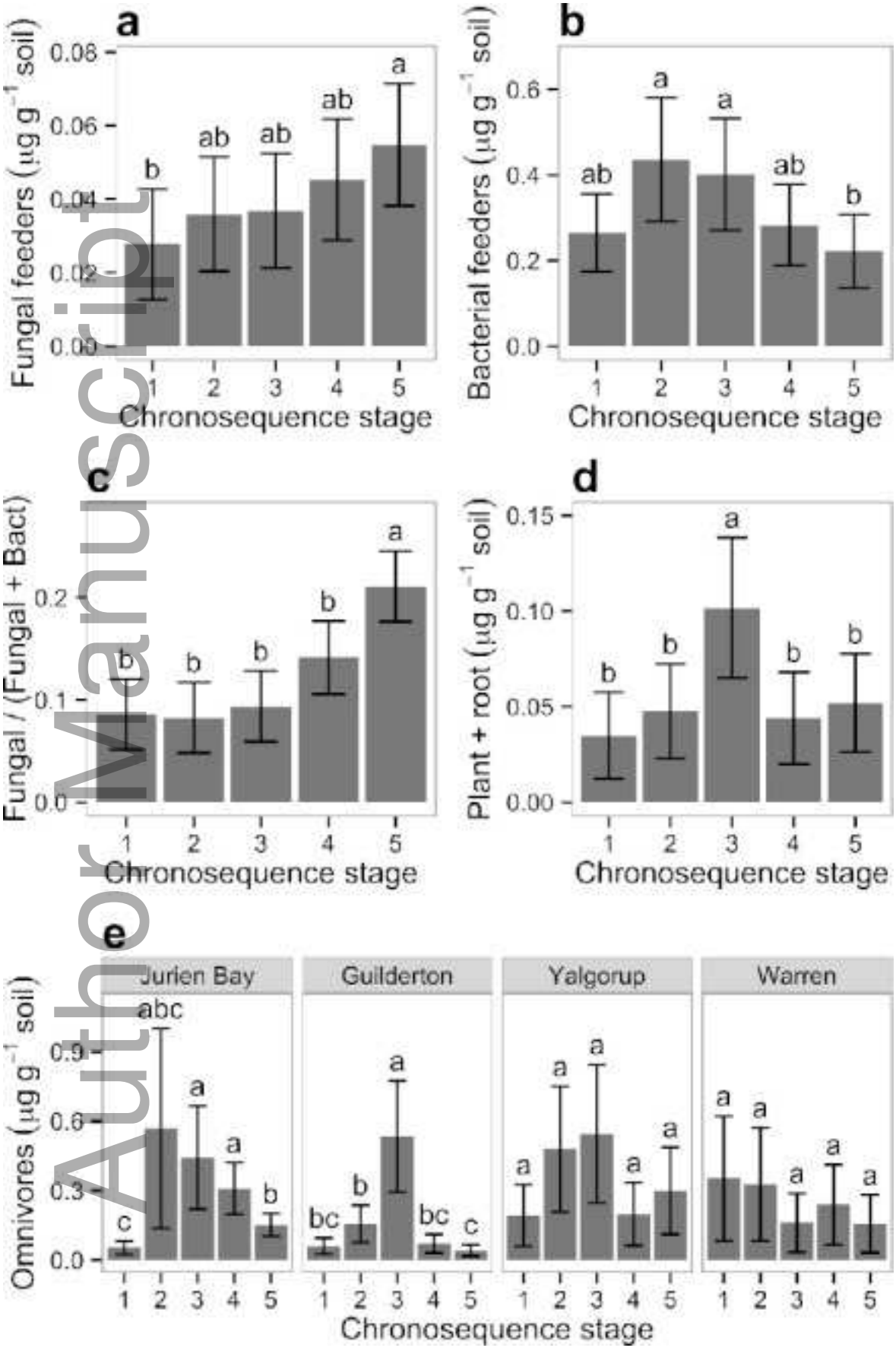

ele_12823_f4.tif

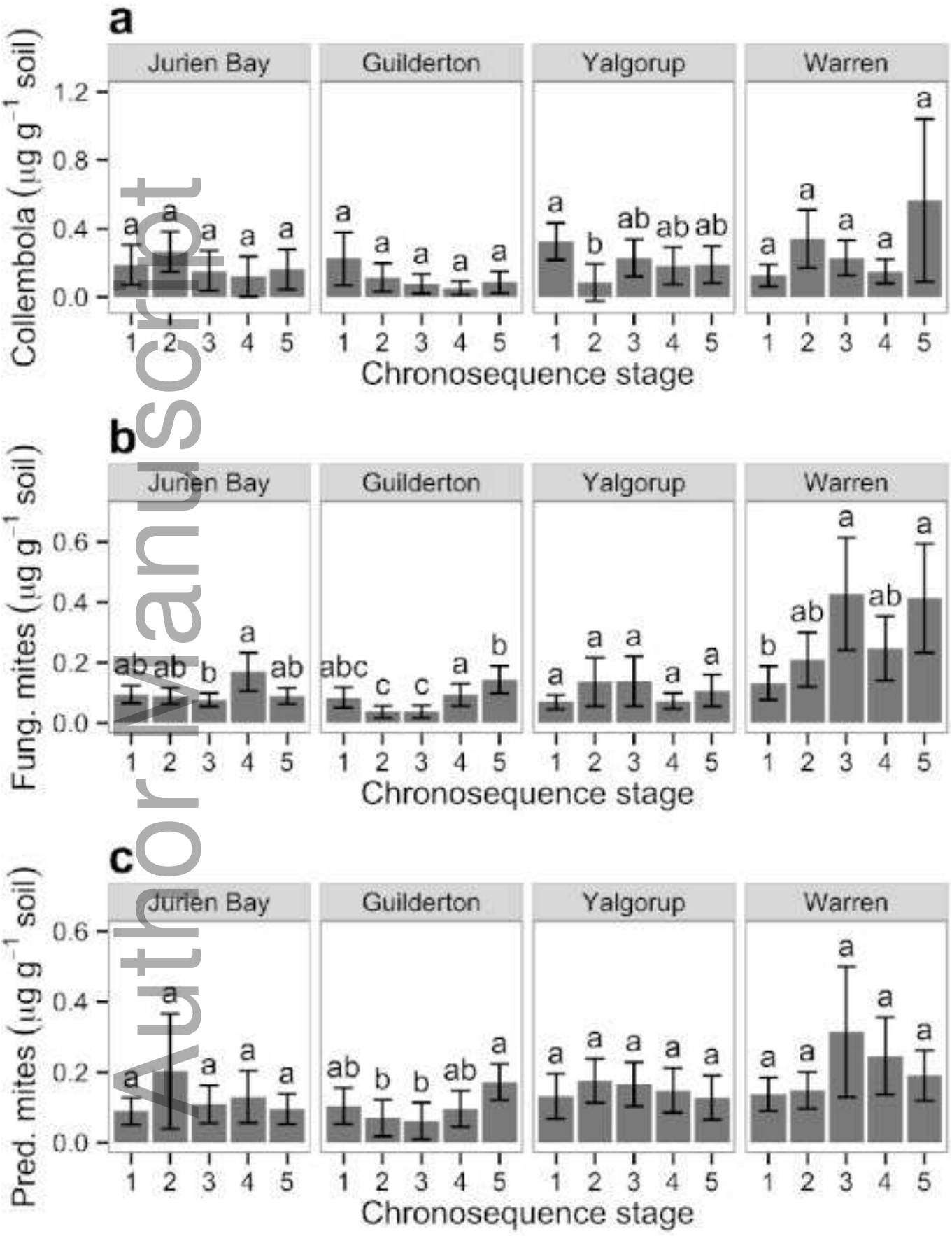

ele_12823_f5.tif

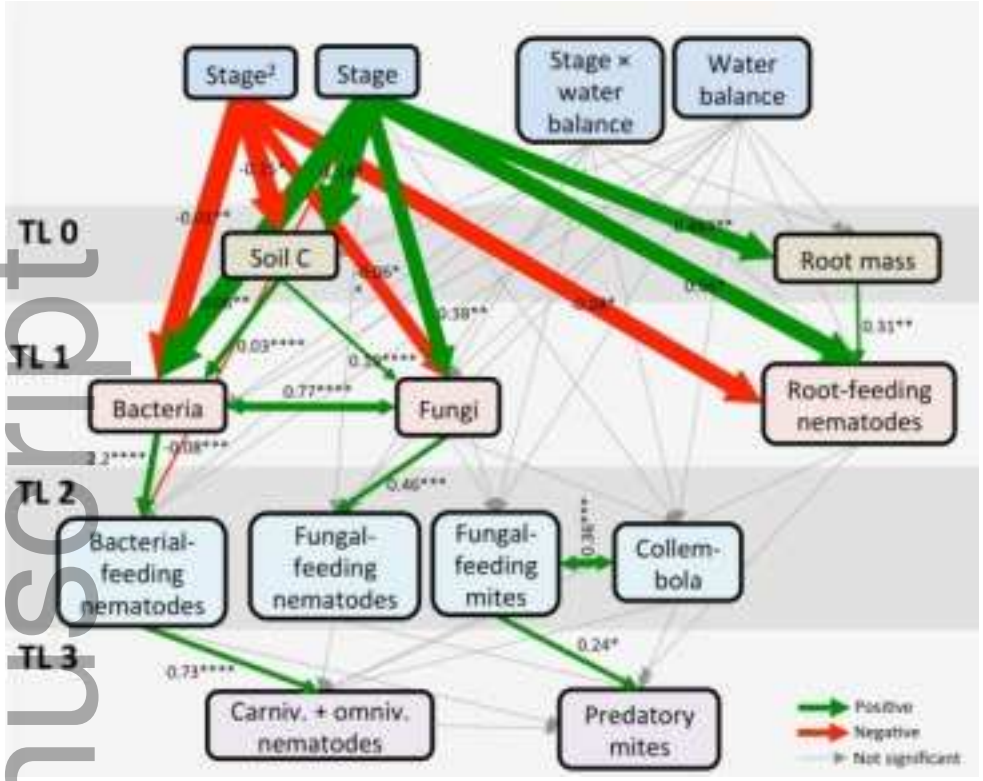

ele_12823_f6.tif